

Proportional and Integral controller based LFC in a Restructured Power System considering Hydrogen Energy Storage Unit with the Computation of Ancillary Service Requirement Assessment Indices

ND. Sridhar*

*Assistant Professor, Department of Electrical Engineering, Annamalai University, Annamalainagar, Tamilnadu, India

Email: sridarnd1@gmail.com

ABSTRACT

This paper proposes the computation procedure for obtaining Power System Ancillary Service Requirement Assessment Indices (PSASRAI) for a Two-Area Thermal Reheat Interconnected Power System (TATRIPS) in a restructured environment. These Indices indicates the Ancillary Service Requirement to improve the efficiency of the physical operation of the power system. Even though Proportional and Integral (PI) type controllers have wide usages in controlling the Load Frequency Control (LFC) problems the Integral gain in the PI controller is limited relatively to small values because of its high the overshoot in the transient's response. Sothe Proportional and Integral plus (PI⁺) controller was proposed and adopted in this paper. The PI⁺ controller uses a low-pass filter on the command signal to remove the over shoot. The PI⁺ controller gains values for the restructured power system are obtained using Bacterial Foraging Optimization (BFO) algorithm. These controllers are implemented in a TATRIPS to achieve a faster restoration time in the output responses of the system when the system experiences various step load perturbations. The PSASRAI are computed based on the settling time and peak over shoot of the control input deviations of each area. To ensure a faster settling time and reduced peak over shoot of the control input requirements, energy storage is an attractive option to adopt for the demand side management implementation. HenceHydrogen Energy Storage (HES)unit was adapted effectively to TATRIPS to meet the peak demand by computing and enhanced Power System Ancillary Service Requirement Assessment Indices. In this paper the PSASRAI are calculated for different types of transactions and the necessary remedial measures to be adopted are also suggested.

Keywords: Ancillary Service, Hydrogen Energy Storage, Proportional and Integral plus Controller, Bacterial Foraging Optimization, Power System Ancillary Service Requirement Assessment Indices.

I. INTRODUCTION

The successful operation of an interconnected power system requires in matching the total generation with total load demand and associated system losses. A small load fluctuation in any area causes the frequency deviation in all the areas and also of the tie-line power flow. These deviations have to be corrected through supplementary control which is referred as LFC and the main objective of the LFC is to maintain the frequency and power interchanges within the interconnected control areas at the scheduled values [1]. The restructuring and deregulation of power

sector is to create a competitive environment where generation and transmission services are bought and sold under demand and supply market conditions. In the deregulated power system, the power generating units are separated from transmission and distribution entities [2- 4] and all the power generating stations are recognized as Independent Power Producers (IPPs) or GENCOs which will have a free market to compete each other to sell the electrical power. The retail consumers are supposed to buy the electrical power from the distribution companies which are referred as DISCOs. In the deregulated power system structure, a distribution company has the freedom to have a

contract with any generation companies for purpose of transaction of power. The different companies may have the bilateral transactions and these will have to be monitored through an independent system operator which will control the number of ancillary services. The main task of the LFC is to maintain the reliability of the system at the desired frequency even to the varying load demand. The generation companies in restructured environment may or may not participate in the LFC task. As far as the optimal LFC schemes for interconnected power systems operating in deregulated environment are concerned, a considerable work has been reported in literature [2-9]. As the distribution companies may have contract with generation companies in its area or other areas for the transaction of power under the supervision of the Independent System Operators (ISO) and the studies try to modify the conventional LFC system to take into account the effect of bilateral contracts on the dynamics and improve the dynamic and transient response of the system under various operating conditions.

Ancillary services can be defined as a set of activities undertaken by generators, consumers and network service providers and coordinated by the system operator that have to maintain the availability and quality of supply. In a competitive power market, various service markets are adopted for ensuring the ancillary services such for voltage support, regulation, etc [10, 11]. The real power generating capacity related ancillary services, including Regulation Down Reserve (RDR), Regulation Up Reserve (RUR) in which regulation is the load following capability under LFC. Spinning Reserve (SR) is a type of operating reserve, which is a resource capacity synchronized to the system that is unloaded, is able to respond immediately to serve load, and is fully available within ten minutes. But Non Spinning Reserve (NSR) are the one in which NSR is not synchronized to the system and Replacement Reserve (RR) is a resource capacity non-synchronized to the system, which is able to serve load normally within thirty or sixty minutes. Reserves can be provided by generating units or interruptible load in some cases [11].

Now-a-days the complexities in the power system are being solved with the use of Evolutionary Computation (EC) such as Bacterial Foraging Optimization (BFO) which mimics how bacteria forage over a landscape of nutrients to perform parallel non-gradient optimization. The BFO algorithm is a computational intelligence based technique that is not affected larger by the size and nonlinearity of the problem and can be convergence to the optimal solution in many problems where most analytical methods fail to converge. This more recent and powerful evolutionary computational technique BFO [18-20] is found to be user friendly and is adopted for simultaneous optimization of several parameters for both primary and secondary control loops of the governor. In this study, BFO algorithm is used to optimize the Proportional and Integral plus (PI+) controller gains for the load frequency control of a TATRIPS in a restructured environment with and without HES unit. Various case studies are analyzed to develop PSASRAI namely, FAI and CAI which are able to predict the modes of power system i.e., normal operating mode, emergency mode and restorative modes.

II. Hydrogen Energy Storage (HES) Systems

The optimization schedule of any distributed energy sources depends on the constraints of the problem, which are load limits, actual generation capabilities, status of the battery, forecasted production schedule. Hydrogen is a serious contender for future energy storage due to its versatility and consequently, producing hydrogen from renewable resources using electrolysis is currently the most desirable objective available. Hydrogen is one of the promising alternatives that can be used as an energy carrier. Essential elements of a hydrogen energy storage system comprise an electrolyzer unit, which converts electrical energy input into hydrogen by decomposing water molecules, the hydrogen storage system itself and a hydrogen energy conversion system, which converts the stored chemical energy in the hydrogen back to electrical energy as shown in Fig 3. The transfer function of AE can be expressed as first order lag:

$$G_{AE}(s) = \frac{K_{AE}}{1 + sT_{AE}} \quad (1)$$

III. Fuel Cell for Energy Storage with Aqua Electrolyze

Fuel cells are static energy conversion device, which are considered to be an important resource in hybrid distributed power system due to the advantages like high efficiency, low pollution etc. An electrolyzer uses electrolysis to breakdown water into hydrogen and oxygen. The oxygen is dissipated into the atmosphere and the hydrogen is stored so it can be used for future generation. A fuel cell converts stored chemical energy, in this case hydrogen, directly into electrical energy. A fuel cell consists of two electrodes that are separated by an electrolyte as shown in Fig 2. Hydrogen is passed over the anode (negative) and oxygen is passed over the cathode (positive) causing hydrogen ions and electrons to form at the anode. The energy produced by the various types of cells depends on the operation temperature, the type of fuel cell and the catalyst used. Fuel cells do not produce any pollutants and have no moving parts.

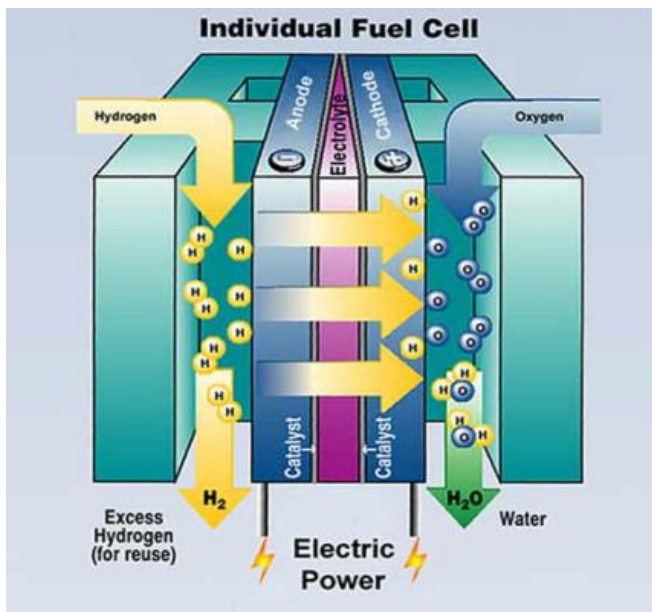


Fig 1. Structure of a fuel cell

The transfer function of Fuel Cell (FC) can be given by a simple linear equation as

$$G_{FC}(s) = \frac{K_{FC}}{1 + sT_{FC}} \quad (2)$$

The overall transfer function of hydrogen Energy storage unit has can be

$$G_{HES}(s) = \frac{K_{HES}}{1 + sT_{HES}} = \frac{K_{AE}}{1 + sT_{AE}} * \frac{K_{FC}}{1 + sT_{FC}} \quad (3)$$

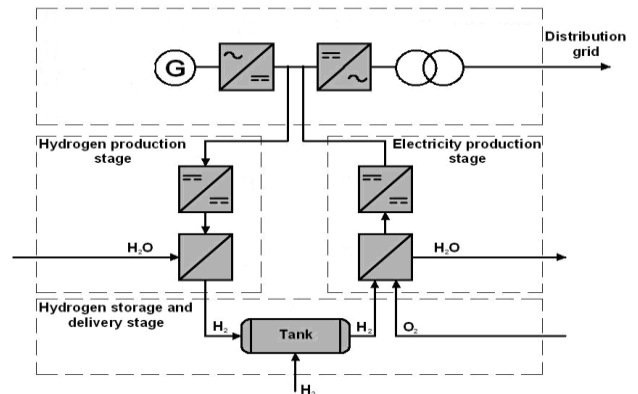


Fig 2. Block diagram of the hydrogen storage unit

i. Control design of Hydrogen Energy Storage unit

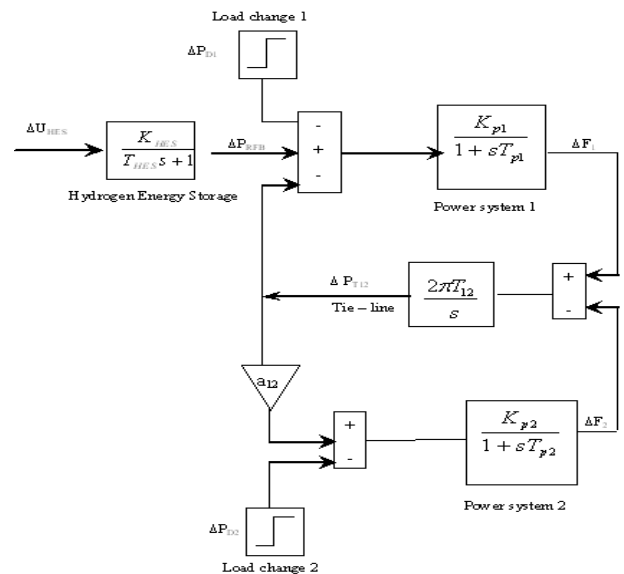


Fig. 3 Linearized reduction model for the control design

The HES unit is modelled as an active power source to area 1 with a time constant T_{HES} , and gain constant K_{HES} . Assuming the time constants T_{HES} is regarded as 0 sec for the control design [9], then the state equation of the system represented by Fig. 4 becomes

$$\begin{bmatrix} \Delta \dot{F}_1 \\ \Delta \dot{F}_{T12} \\ \Delta \dot{F}_2 \end{bmatrix} = \begin{bmatrix} -\frac{1}{T_{p1}} & -\frac{K_{p1}}{T_{p1}} & 0 \\ 2\pi T_{12} & 0 & -2\pi T_{12} \\ 0 & \frac{a_{12} k_{p2}}{T_{p2}} & -\frac{1}{T_{p2}} \end{bmatrix} \begin{bmatrix} \Delta F_1 \\ \Delta P_{T12} \\ \Delta F_2 \end{bmatrix} + \begin{bmatrix} \frac{k_{p1}}{T_{p1}} \\ 0 \\ 0 \end{bmatrix} [\Delta P_{HES}] \quad (4)$$

The equivalent system is derived by assuming the synchronizing coefficient T_{12} to be large. From the state equation of $\Delta \dot{F}_{T12}$ in Eq (12)

$$\frac{\Delta \dot{F}_{T12}}{2\pi T_{12}} = \Delta F_1 - \Delta F_2 \quad (5)$$

Setting the value of T_{12} in Eq (13) to be infinity yields $\Delta F_1 = \Delta F_2$. Next, by multiplying state equation of

Δf_1 and Δf_2 by $\frac{T_{p1}}{k_{p1}}$ and $\frac{T_{p2}}{a_{12} k_{p2}}$ respectively, Where $A = \left(-\frac{1}{k_{p1}} - \frac{1}{k_{p2} a_{12}} \right) / \left(\frac{T_{p1}}{k_{p1}} + \frac{T_{p2}}{k_{p2} a_{12}} \right)$,

then

$$\frac{T_{p1}}{k_{p1}} \Delta f_1 = -\frac{1}{k_{p1}} \Delta F_1 - \Delta P_{T12} + \Delta P_{HES} \quad (14)$$

$$\frac{T_{p2}}{a_{12} k_{p2}} \Delta f_2 = \frac{-1}{k_{p2} a_{12}} \Delta F_2 + \Delta P_{T12} \quad (6)$$

By summing Eq (14) and Eq (15) and using the above relation $\Delta F_1 = \Delta F_2 = \Delta F$

$$\Delta f = \left(\frac{-\frac{1}{k_{p1}} - \frac{1}{k_{p2} a_{12}}}{\frac{T_{p1}}{k_{p1}} + \frac{T_{p2}}{k_{p2} a_{12}}} \right) \Delta F + \frac{1}{\left(\frac{T_{p1}}{k_{p1}} + \frac{T_{p2}}{k_{p2} a_{12}} \right)} \Delta P_{HES} + C \Delta P_D \quad (7)$$

Where ΔP_D is the load change in this system and the control $\Delta P_{HES} = -K_{HES} \Delta F$ is applied then.

$$\Delta F = \frac{C}{s + A + K_{HES} B} \Delta P_D \quad (8)$$

$$B = \frac{1}{\left[\frac{T_{p1}}{K_{p1}} + \frac{T_{p2}}{K_{p2} a_{12}} \right]}$$

Where C is the proportionality constant between change in frequency and change in load demand. In Eq (17) the final values with $K_{HES} = 0$ and with $K_{HES} \neq 0$ are C/A and $C/(A + K_{HES} B)$ respectively therefore the percentage reduction is represented by

$$C/(A + K_{HES} B) / (C/A) = R/100 \quad (9)$$

For a given R, the control gain of HES is calculated as

$$K_{HES} = \frac{A}{BR} (100 - R) \quad (10)$$

The linearized model of an interconnected two-area reheat thermal power system in deregulated environment is shown in Fig.4 after incorporating HES unit with FC.

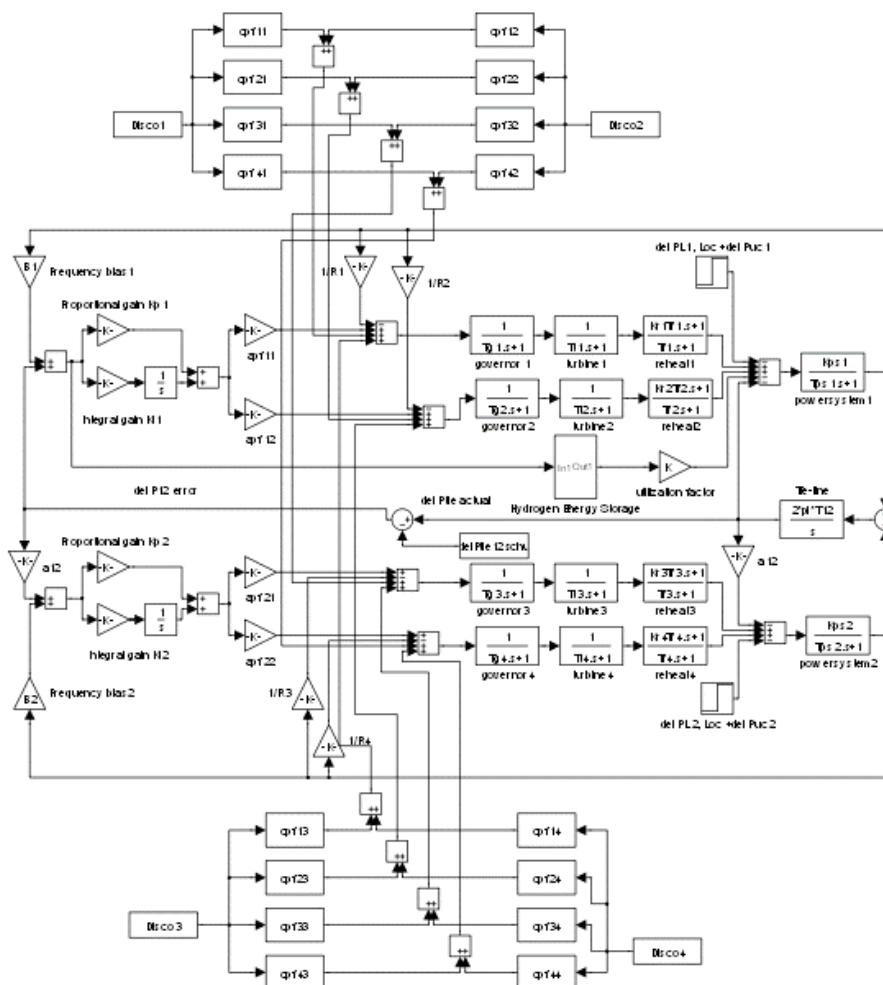


Fig. 4 Simulink model of a TATRIPS in restructured environment with HES unit and Fuel Cell.

IV. Design of decentralized PI⁺ controllers

In PI controller, K_P provides stability and high frequency response and K_I ensures that the average error is driven to zero. So no long term error, as the two gains are tuned. This normally provides high

responsive systems. But the predominant weakness of PI controller is it often produces excessive overshoot to a step command. The PI controller lacks a windup function to control the integral value during saturation. But PI⁺ uses a low pass filter on the command signal to limit the overshoot.

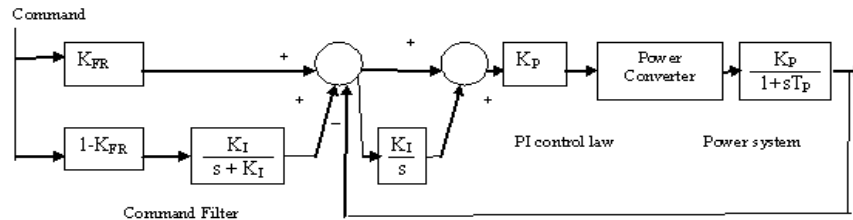


Fig.5 Block diagram for PI⁺ control

The PI⁺ controller is shown in Fig 6. The system is the PI controller with a command filter added. The degree to which a PI⁺ controller filters the command signal is determined by the gain K_{FR} . When K_{FR} is 1, all filtering is removed and the controller is identical to a PI controller. Filtering is most severe when K_{FR} is zero. When K_{FR} is zero, command is filtered by $K_I/(s + K_I)$, which is a single-pole low-pass filter at the frequency K_I (in rad/sec). This case will allow the highest integral gain but also will most severely limit the controller command response. Typically, $K_{FR} = 0$ will allow an increase of almost three times in the integral gain but will reduce the bandwidth by about one-half when compared with $K_{FR} = 1$ (PI control). Finding the optimal value of K_{FR} depends on the application, but a value of 0.65 has been found to work in many applications. This value typically allows the integral gain to more than double while reducing the bandwidth by only 15%-20% [17]. K_I as the frequency of the command low-pass filter because it is excellent at canceling the peaking caused by the integral gain. PI⁺ control is that it uses the command filter to attenuate the peaking caused by PI. The peaking caused by K_I can be cancelled by the attenuation of a low-pass filter with a break of K_I . In fig.6 the control law for PI⁺ controller is represented as

$$Control = K_p \left(command \left(K_{FR} + (1 - K_{FR}) \frac{K_I}{s + K_I} \right) - Feedback \right) \left(1 + \frac{K_I}{s} \right) \quad (11)$$

In PI⁺ is often referred as Pseudo Derivative Feedback with Feed forward (PDFF) is shown in Fig7 and the control law for PI⁺ controller is represented as

$$Control = K_p \left((command - Feedback) \frac{K_I}{s} + K_{FR} command - Feedback \right) \quad (12)$$

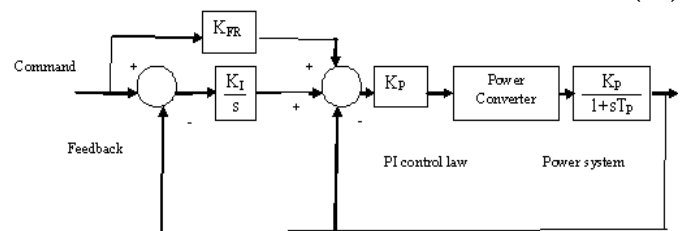


Fig 6 Pseudo Derivative Feedback with Feed forward (PDFF) controller

PDFF is an alternative way to implement PI⁺; it is useful in digital systems because there are no multiplications before the integral. Multiplication, when not carefully constructed, causes numerical noise. That noise prior to the integrator may cause drift in the control loop as the round-off error accumulates in the integrator. PDFF has a single operation, a subtraction, which is usually noiseless, before the integration and thus easily avoids such noise.

V. Bacterial Foraging Optimization (BFO) Technique

BFO method was introduced by Passino [18] motivated by the natural selection which tends to eliminate the animals with poor foraging strategies and favour those having successful foraging strategies. The foraging strategy is governed by four processes

namely Chemotaxis, Swarming, Reproduction and Elimination and Dispersal. Chemotaxis process is the characteristics of movement of bacteria in search of food and consists of two processes namely swimming and tumbling. A bacterium is said to be swimming if it moves in a predefined direction, and tumbling if it starts moving in an altogether different direction. To represent a tumble, a unit length random direction $\phi(j)$ is generated. Let, “j” is the index of chemotactic step, “k” is reproduction step and “l” is the elimination dispersal event. $\theta_i(j, k, l)$, is the position of i^{th} bacteria at j^{th} chemotactic step k^{th} reproduction step and l^{th} elimination dispersal event. The position of the bacteria in the next chemotactic step after a tumble is given by

$$\theta^i(j+1, k, l) = \theta^i(j, k, l) + C(i) \phi(j) \quad (13)$$

If the health of the bacteria improves after the tumble, the bacteria will continue to swim to the same direction for the specified steps or until the health degrades. Bacteria exhibits swarm behavior i.e. healthy bacteria try to attract other bacterium so that together they reach the desired location (solution point) more rapidly. The effect of swarming is to make the bacteria congregate into groups and moves as concentric patterns with high bacterial density [18]. Mathematically swarming behavior can be modelled.

$$J_{cc}(\theta, P(j, k, l)) = \sum_{i=1}^S J_{cc}^i(\theta, \theta^i(j, k, l))$$

$$= \sum_{i=1}^S \left[-d_{attract} \exp(-\omega_{attract}) \sum_{m=1}^P (\theta^m - \theta_m^i)^2 \right]$$

$$+ \sum_{i=1}^S \left[-h_{repellent} \exp(-\omega_{repellent}) \sum_{m=1}^P (\theta^m - \theta_m^i)^2 \right] \quad (14)$$

J_{cc} is Relative distance of each bacterium from the fittest bacterium, S is Number of bacteria, P is Number of parameters to be optimized, θ^m is Position of the fittest bacteria, $d_{attract}$, $\omega_{attract}$, $h_{repellent}$, $\omega_{repellent}$ - different co-efficients representing the swarming behaviour of the bacteria which are to be chosen properly. In Reproduction step, population members who have sufficient nutrients will reproduce and the least healthy bacteria will die. The healthier population replaces unhealthy bacteria, which get eliminated owing to their poorer foraging abilities. This makes the population of bacteria constant in the evolution process. In this process a sudden unforeseen event may drastically alter the evolution and may cause the elimination and / or dispersal to a new environment. Elimination and dispersal helps in reducing the behavior of stagnation i.e., being trapped in a premature solution point or local optima. The flow chat of BFO algorithm is shown in Fig 7

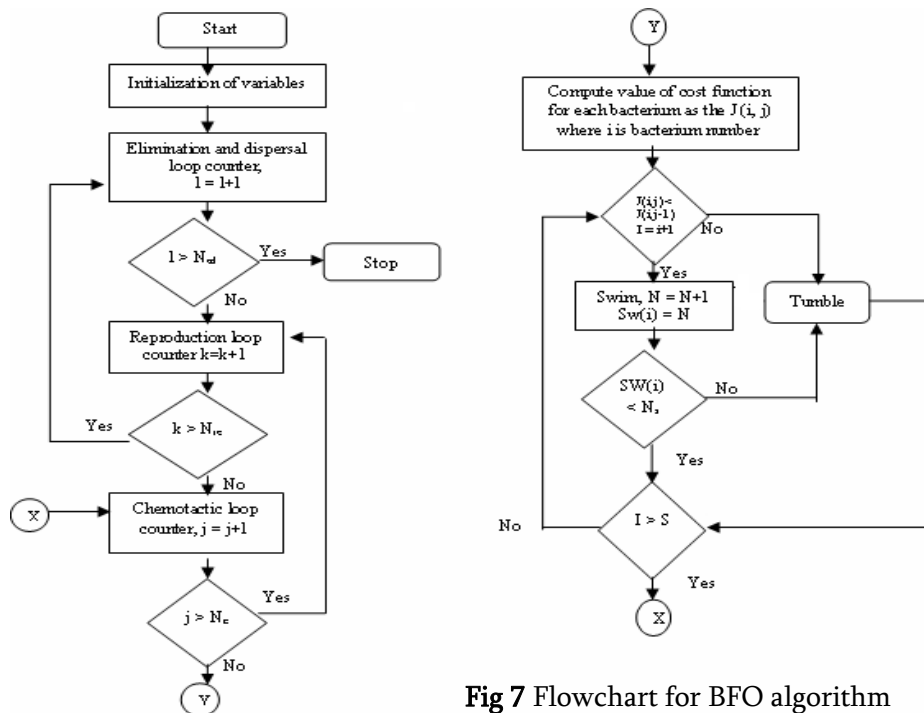


Fig 7 Flowchart for BFO algorithm

VI. Simulation Results and Observations

The Two-Area Thermal Reheat Interconnected Restructured Power System considered for the study consists of two GENCOs and two DISCOs in each area. The nominal parameters are given in Appendix. The optimal solution for the objective function (25) is obtained using the frequency deviations of control BFO algorithm by optimizing the solutions of control inputs for the various case studies as shown in Table 1 and 2. The results are obtained by MATLAB 7.01 software and 100 iterations are chosen for the convergence of the solution using BFO algorithm. These PI⁺ controllers are implemented in a Two-Area Thermal Reheat Interconnected Restructured Power System considering HES with Fuel Cell unit considering different utilization of capacity (K= 0, 0.25, 0.5, 0.75, 1.0) and for different type of transactions. The corresponding frequency deviations (Δf), tie- line power deviation (ΔP_{tie}) and control input deviations (ΔP_c) are obtained with respect to time as shown in Fig 9-10. Simulation results reveal that the proposed PI⁺ controller for the restructured power system coordinated with HES and fuel cell units greatly reduces the peak over shoot / under shoot of the frequency deviations and tie- line power flow deviation. And also it reduces the control input requirements and the settling time of the output responses are also reduced considerably is shown in Table 3.

i. PSASRAI

a) Based on Settling Time

- (i) If then the integral controller gain of each control area has to be increased causing the
- (ii) speed changer valve to open up widely. Thus the speed- changer position attains a constant value only when the frequency error is reduced to zero.

areas and tie- line power changes. The gain values of HES with fuel cell (K_{HES}) are calculated using Eq (19) for the given value of speed regulation coefficient (R). The gain value is of the HES with fuel cell is found to be $K_{RFB} = 0.67$. The PI⁺ controller gains (K_p, K_i) are tuned with

- (iii) If $1.0 < \varepsilon_1, \varepsilon_2, \varepsilon_5, \varepsilon_6 \leq 1.5$ then more amount of distributed generation requirement is needed. Energy storage is an attractive option to augment demand side management implementation by ensuring the Ancillary Services to the power system.
- (iv) If $\varepsilon_1, \varepsilon_2, \varepsilon_5, \varepsilon_6 \geq 1.5$ then the system is vulnerable and the system becomes unstable and may even result to blackouts.

b) Based on peak undershoot

- (i) If $0.15 \leq \varepsilon_3, \varepsilon_4, \varepsilon_7, \varepsilon_8 < 0.2$ then Energy Storage Systems (ESS) for LFC is required as the conventional load-frequency controller may no longer be able to attenuate the large frequency oscillation due to the slow response of the governor for unpredictable load variations. A fast-acting energy storage system in addition to the kinetic energy of the generator rotors is advisable to damp out the frequency oscillations.
- (ii) If $0.2 \leq \varepsilon_3, \varepsilon_4, \varepsilon_7, \varepsilon_8 < 0.3$ then more amount of distribution generation requirement is required or Energy Storage Systems (ESS) coordinated control with the FACTS devices are required for the improvement relatively stability of the power system in the LFC application and the load shedding is also preferable
- (iii) If $\varepsilon_3, \varepsilon_4, \varepsilon_7, \varepsilon_8 > 0.3$ then the system is vulnerable and the system becomes unstable and may result to

(v) blackout

Table 1 Optimized Controller parameters of the TATRIPS using PI⁺ controller

TATRIPS with HES unit	Controller gain of AREA 1 With $K_{FR} = 0.65$		Controller gain of AREA 2 With $K_{FR} = 0.65$	
	K_{p1}	K_{i1}	K_{p2}	K_{i2}
Case 1	0.228	0.496	0.102	0.124
Case 2	0.252	0.512	0.127	0.131
Case 3	0.287	0.545	0.134	0.145
Case 4	0.296	0.562	0.142	0.213
Case 5	0.328	0.575	0.154	0.236
Case 6	0.241	0.696	0.138	0.296
Case 7	0.283	0.702	0.148	0.334
Case 8	0.378	0.764	0.152	0.386
Case 9	0.398	0.791	0.165	0.375
Case 10	0.402	0.798	0.223	0.381
Case 11	0.427	0.856	0.286	0.393
Case 12	0.494	0.886	0.264	0.396
Case 13	0.538	0.825	0.271	0.462
Case 14	0.591	0.846	0.288	0.476

Table 2 Optimized Controller parameters of the TATRIPS with HES unit using PI⁺ controller

TATRIPS (Poolco based transaction)	Setting time (τ_s) in sec			Peak over / under shoot		
	ΔF_1	ΔF_2	ΔP_{tie}	ΔF_1 in Hz	ΔF_2 in Hz	ΔP_{tie} in p.u.MW
PI controller	18.14	17.52	20.13	0.321	0.215	0.082
PI ⁺ controller	13.21	15.19	17.53	0.253	0.171	0.062
PI ⁺ controller with HES unit	2.447	2.912	5.135	0.097	0.036	0.015

Table 3 Comparison of the system dynamic performance for TATRIPS

TATRIPS	Controller gain of AREA 1 With $K_{FR} = 0.65$		Controller gain of AREA 2 With $K_{FR} = 0.65$	
	K_{p1}	K_{i1}	K_{p2}	K_{i2}
Case 1	0.341	0.519	0.191	0.105
Case 2	0.384	0.412	0.212	0.125
Case 3	0.428	0.485	0.236	0.133
Case 4	0.396	0.459	0.242	0.142
Case 5	0.412	0.486	0.253	0.146
Case 6	0.316	0.543	0.121	0.209
Case 7	0.336	0.585	0.139	0.201
Case 8	0.341	0.595	0.218	0.192
Case 9	0.357	0.593	0.247	0.258
Case 10	0.364	0.632	0.274	0.242
Case 11	0.384	0.623	0.277	0.198
Case 12	0.401	0.674	0.279	0.236
Case 13	0.419	0.687	0.286	0.253
Case 14	0.462	0.693	0.296	0.258

Table 4(a) FAI without and with HES unit (utilization factor K=1) for TATRIPS using PI⁺ controller

TATRIPS	Feasible Assessment Indices (FAI) based on control input deviations (ΔP_c) without HES unit (utilization factor K=0)					Feasible Assessment Indices (FAI) based on control input deviations (ΔP_c) with HES unit (utilization factor K=0.75)				
	ε_1	ε_2	ε_3	ε_4	$\int P_{C1}$	ε_1	ε_2	ε_3	ε_4	$\int P_{HES}$
Case 1	0.912	0.856	0.123	0.014	1.011	0.861	0.796	0.078	0.010	0.468
Case 2	1.045	0.942	0.205	0.024	1.125	0.875	0.801	0.112	0.011	0.469
Case 3	1.264	1.006	0.281	0.036	2.662	0.877	0.913	0.123	0.014	0.525
Case 4	1.065	1.235	0.211	0.049	0.712	0.959	0.974	0.135	0.018	0.558
Case 5	1.351	1.278	0.295	0.064	2.857	1.201	1.105	0.248	0.044	0.451
Case 6	0.916	0.871	0.131	0.078	1.131	0.802	0.775	0.119	0.053	0.468
Case 7	1.105	0.908	0.204	0.082	1.221	0.928	0.886	0.136	0.073	0.528
Case 8	1.112	1.014	0.304	0.097	2.236	0.936	0.941	0.206	0.081	0.517
Case 9	1.224	1.235	0.208	0.167	1.016	0.938	1.049	0.178	0.149	0.545
Case 10	1.338	1.263	0.315	0.182	2.253	1.100	1.121	0.275	0.156	0.583

Table 4(b)- FAI without and with HES unit (utilization factor K=0.75) for TATRIPS using PI⁺ controller

TATRIPS	Feasible Assessment Indices (FAI) based on control input deviations (ΔP_c) without HES unit (utilization factor K=0)					Feasible Assessment Indices (FAI) based on control input deviations (ΔP_c) with HES unit (utilization factor K=1)				
	ε_1	ε_2	ε_3	ε_4	$\int P_{C1}$	ε_1	ε_2	ε_3	ε_4	$\int P_{HES}$
Case 1	0.912	0.856	0.123	0.014	1.011	0.801	0.704	0.082	0.006	0.534
Case 2	1.045	0.942	0.205	0.024	1.125	0.803	0.772	0.095	0.008	0.564
Case 3	1.264	1.006	0.281	0.036	2.662	0.806	0.882	0.114	0.010	0.591
Case 4	1.065	1.235	0.211	0.049	0.712	0.914	0.911	0.118	0.013	0.596
Case 5	1.351	1.278	0.295	0.064	2.857	1.025	1.061	0.219	0.039	0.462
Case 6	0.916	0.871	0.131	0.078	1.131	0.795	0.698	0.098	0.051	0.486
Case 7	1.105	0.908	0.204	0.082	1.221	0.863	0.884	0.123	0.068	0.531
Case 8	1.112	1.014	0.304	0.097	2.236	0.904	0.939	0.186	0.071	0.562
Case 9	1.224	1.235	0.208	0.167	1.016	0.831	1.021	0.152	0.141	0.608
Case 10	1.338	1.263	0.315	0.182	2.253	1.002	1.085	0.245	0.153	0.628

Table 4(c)- FAI without and with HES unit (utilization factor K=0.5) for TATRIPS using PI⁺ controller

TATRIPS	Comprehensive Assessment Indices (CAI) based on control input deviations (ΔP_c) without HES unit (utilization factor K=0)					Comprehensive Assessment Indices (CAI) based on control input deviations (ΔP_c) with HES unit (utilization factor K=1)				
	ε_5	ε_6	ε_7	ε_8	$\int P_{C1}$	ε_5	ε_6	ε_7	ε_8	$\int P_{HES}$
Case 11	1.125	1.423	0.341	0.286	1.098	1.001	1.237	0.301	0.235	0.498
Case 12	1.511	1.411	0.378	0.335	3.188	1.081	1.343	0.310	0.301	0.594
Case 13	1.323	1.526	0.425	0.486	1.785	1.001	1.418	0.371	0.417	0.571
Case 14	1.536	1.635	0.451	0.508	3.172	1.427	1.551	0.382	0.474	0.588

Table 4(d)– FAI without and with HES unit (utilization factor K=0.25) for TATRIPS using PI⁺ controller

TATRIPS	Feasible Assessment Indices (FAI) based on control input deviations (ΔP_c) without HES unit (utilization factor K=0)					Feasible Assessment Indices (FAI) based on control input deviations (ΔP_c) with HES unit (utilization factor K=0.5)				
	ε_1	ε_2	ε_3	ε_4	$\int P_{C1}$	ε_1	ε_2	ε_3	ε_4	$\int P_{HES}$
Case 1	0.912	0.856	0.123	0.014	1.011	0.855	0.781	0.100	0.010	0.425
Case 2	1.045	0.942	0.205	0.024	1.125	0.871	0.808	0.128	0.018	0.448
Case 3	1.264	1.006	0.281	0.036	2.662	0.900	0.916	0.139	0.020	0.521
Case 4	1.065	1.235	0.211	0.049	0.712	0.945	0.945	0.148	0.021	0.538
Case 5	1.351	1.278	0.295	0.064	2.857	1.179	1.101	0.261	0.052	0.439
Case 6	0.916	0.871	0.131	0.078	1.131	0.798	0.771	0.122	0.062	0.461
Case 7	1.105	0.908	0.204	0.082	1.221	0.928	0.878	0.165	0.071	0.486
Case 8	1.112	1.014	0.304	0.097	2.236	0.935	0.954	0.231	0.078	0.489
Case 9	1.224	1.235	0.208	0.167	1.016	0.923	1.109	0.179	0.158	0.534
Case 10	1.338	1.263	0.315	0.182	2.253	1.100	1.127	0.289	0.162	0.542

Table 5(a)CAI without and with HES unit (utilization factor K=1) for TATRIPS using PI⁺ controller

TATRIPS	Comprehensive Assessment Indices (CAI) based on control input deviations (ΔP_c) without HES unit (utilization factor K=0)					Comprehensive Assessment Indices (CAI) based on control input deviations (ΔP_c) with HES unit (utilization factor K=0.75)				
	ε_5	ε_6	ε_7	ε_8	$\int P_{C1}$	ε_5	ε_6	ε_7	ε_8	$\int P_{HES}$
Case 11	1.125	1.423	0.341	0.286	1.098	1.021	1.331	0.302	0.242	0.447
Case 12	1.511	1.411	0.378	0.335	3.188	1.101	1.410	0.319	0.305	0.528
Case 13	1.323	1.526	0.425	0.486	1.785	1.011	1.498	0.378	0.411	0.541
Case 14	1.536	1.635	0.451	0.508	3.172	1.436	1.598	0.400	0.481	0.547

Table 5(b)CAI without and with HES unit (utilization factor =0.75) for TATRIPS using PI⁺ controller

TATRIPS	Comprehensive Assessment Indices (CAI) based on control input deviations (ΔP_c) without HES unit (utilization factor K=0)					Comprehensive Assessment Indices (CAI) based on control input deviations (ΔP_c) with HES unit (utilization factor K=0.5)				
	ε_5	ε_6	ε_7	ε_8	$\int P_{C1}$	ε_5	ε_6	ε_7	ε_8	$\int P_{HES}$
Case 11	1.125	1.423	0.341	0.286	1.098	1.048	1.312	0.313	0.251	0.385
Case 12	1.511	1.411	0.378	0.335	3.188	1.189	1.421	0.321	0.310	0.448
Case 13	1.323	1.526	0.425	0.486	1.785	1.081	1.540	0.400	0.421	0.328
Case 14	1.536	1.635	0.451	0.508	3.172	1.478	1.611	0.404	0.492	0.467

Table 5(c)CAI without and with HES unit (utilization factor K=0.5) for TATRIPS using PI+ controller

TATRIPS	Feasible Assessment Indices (FAI) based on control input deviations (ΔP_c) without HES unit (utilization factor K=0)					Feasible Assessment Indices (FAI) based on control input deviations (ΔP_c) with HES unit (utilization factor K=0.25)				
	ε_1	ε_2	ε_3	ε_4	$\int P_{C1}$	ε_1	ε_2	ε_3	ε_4	$\int P_{HES}$
	Case 1	0.912	0.856	0.123	0.014	1.011	0.858	0.783	0.110	0.014
Case 2	1.045	0.942	0.205	0.024	1.125	0.901	0.821	0.146	0.016	0.414
Case 3	1.264	1.006	0.281	0.036	2.662	0.951	0.912	0.187	0.024	0.425
Case 4	1.065	1.235	0.211	0.049	0.712	0.961	0.951	0.150	0.040	0.521
Case 5	1.351	1.278	0.295	0.064	2.857	1.293	1.136	0.262	0.061	0.396
Case 6	0.916	0.871	0.131	0.078	1.131	0.810	0.800	0.131	0.067	0.441
Case 7	1.105	0.908	0.204	0.082	1.221	0.943	0.879	0.172	0.082	0.459
Case 8	1.112	1.014	0.304	0.097	2.236	0.956	0.961	0.253	0.086	0.444
Case 9	1.224	1.235	0.208	0.167	1.016	0.936	1.109	0.185	0.171	0.493
Case 10	1.338	1.263	0.315	0.182	2.253	1.200	1.156	0.291	0.180	0.497

Table 5(d)CAI without and with HES unit (utilization factor K=0.25) for TATRIPS using PI+ controller

TATRIPS	Comprehensive Assessment Indices (CAI) based on control input deviations (ΔP_c) without HES unit (utilization factor K=0)					Comprehensive Assessment Indices (CAI) based on control input deviations (ΔP_c) with HES unit (utilization factor K=0.25)				
	ε_5	ε_6	ε_7	ε_8	$\int P_{C1}$	ε_5	ε_6	ε_7	ε_8	$\int P_{HES}$
	Case 11	1.125	1.423	0.341	0.286	1.098	1.065	1.206	0.321	0.261
Case 12	1.511	1.411	0.378	0.335	3.188	1.140	1.284	0.328	0.305	0.420
Case 13	1.323	1.526	0.425	0.486	1.785	1.148	1.451	0.401	0.431	0.438
Case 14	1.536	1.635	0.451	0.508	3.172	1.341	1.529	0.414	0.497	0.445

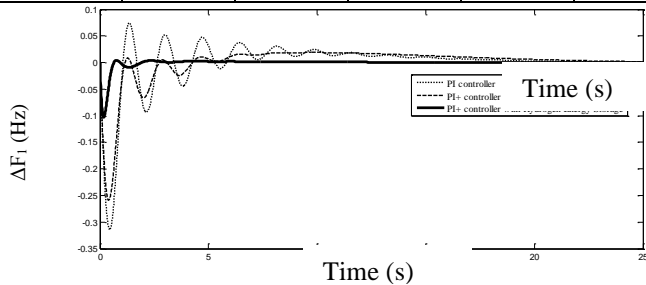


Fig. 9(a) ΔF_1 (Hz) Vs Time (s)

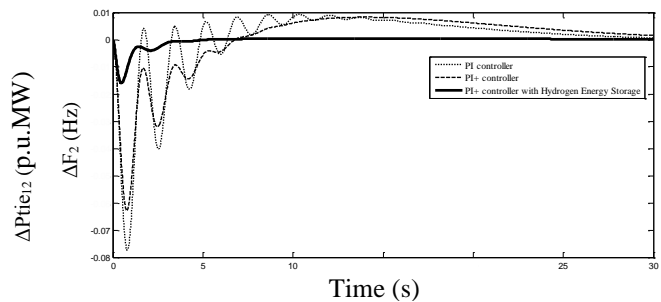


Fig.9 (c) ΔP_{tie12} (p.u.MW) Vs Time (s)

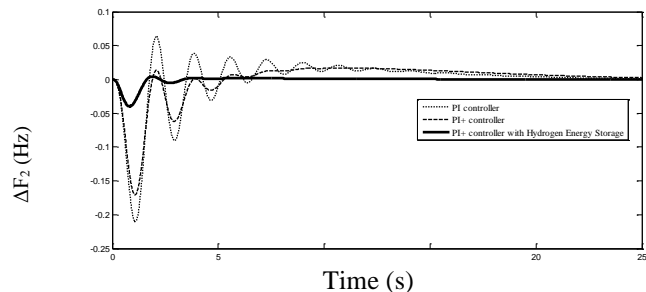


Fig.9 (b) ΔF_2 (Hz) Vs Time (s)

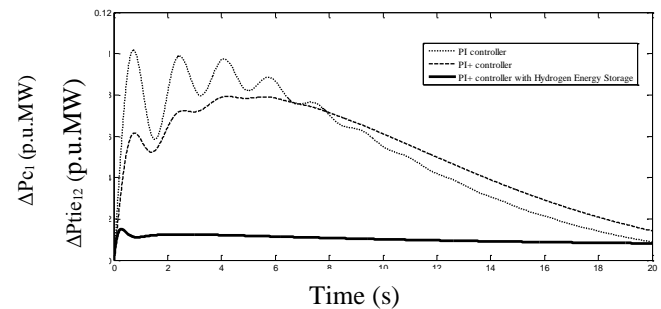


Fig.9 (d) ΔP_{c1} (p.u.MW) Vs Time (s)

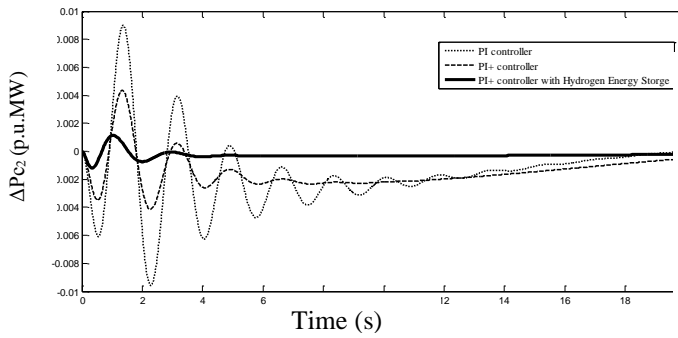


Fig.9 (e) ΔPC_2 (p.u.MW) Vs Time (s)

Fig.9 Dynamic responses of the frequency deviations, tie- line power deviations and Control input deviations for TATRIPS in the restructured scenario-1 (poolco based transactions) using PI+ controller

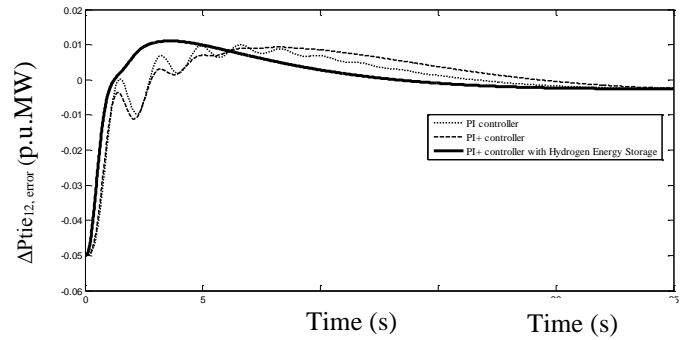


Fig.10 (d) $\Delta Ptie_{12_error}$ (p.u.MW) Vs Time (s)

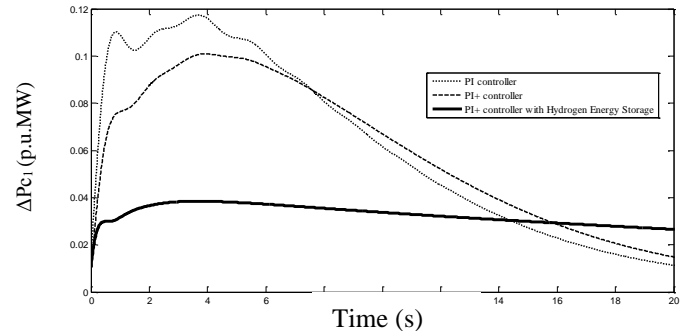


Fig.10 (e) ΔPC_1 (p.u.MW) Vs Time (s)

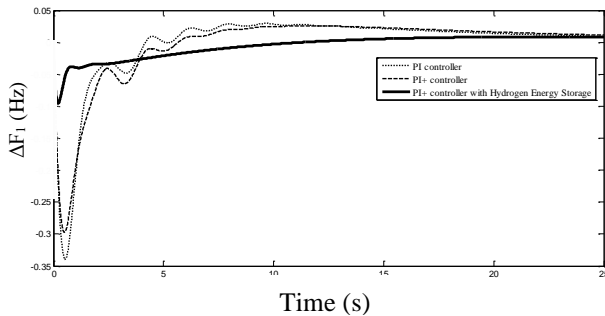


Fig.10 (a) ΔF_1 (Hz) Vs Time (s)

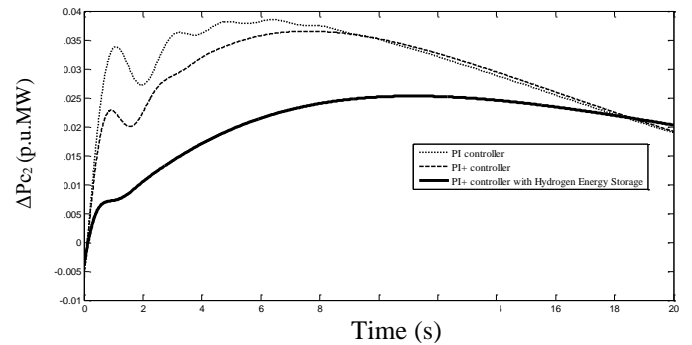


Fig.10 (f) ΔPC_2 (p.u.MW) Vs Time (s)

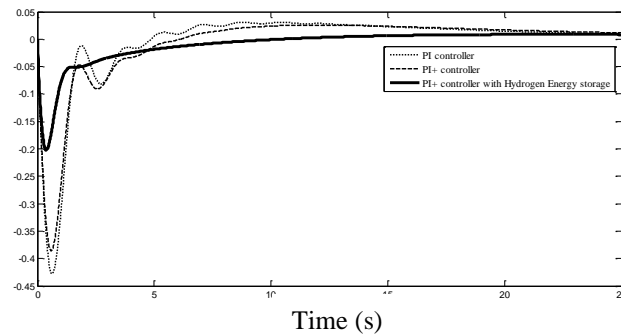


Fig.10 (b) ΔF_2 (Hz) Vs Time (s)

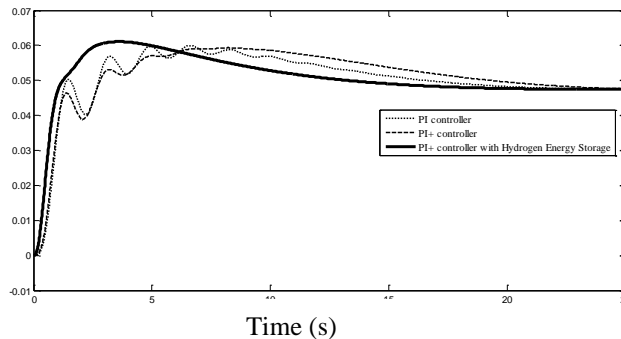


Fig.10 (c) $\Delta Ptie_{12_actual}$ (p.u.MW) Vs Time (s)

Fig.10 Dynamic responses of the frequency deviations, tie- line power deviations, and Control input deviations for TATRIPS in the restructured scenario-2 (bilateral based transactions) using PI+ controller

VI. CONCLUSION

This paper proposes the design of various PSASRAI which highlights the necessary requirements that can be adopted in minimizing the frequency deviations, tie-line power deviation in a TATRIPS in a faster manner to ensure the reliable operation of the power system. The PI+ controllers are designed using BFO algorithm and implemented in a TATRIPS without and with HES unit. As the PI+ control uses a low-pass filter on the command signal to remove overshoot. In

this way, the integral gain can be raised to higher values for the load frequency applications. It has been proved that the PI⁺ controller as it uses the command filter, attenuates the peaking caused by PI controller gains. BFO Algorithm was employed to achieve the optimal parameters of gain values of the various combined control strategies as BFO algorithm is easy to implement without additional computational complexity, with quite promising results and ability to jump out the local optima. Moreover, Power flow control by HES unit is also found to be efficient and effective for improving the dynamic performance of load frequency control of the interconnected power system than that of the system without HES unit. From the simulated results it is observed that the restoration indices calculated for the TATRIPS with HES unit indicates that more sophisticated control for a better restoration of the power system output responses and to ensure improved PSASRAI in order to provide good margin of stability than that of the TATRIPS without HES unit.

VII. REFERENCES

- [1]. H.Shayeghi, H.A.Shayanfar and A. Jalili, "Load frequency control strategies: A state-of-the-art survey for the researcher", *Energy Conversion and Management*, Vol. 50, Issue 2, pp. 344-353, 2009.
- [2]. P. Kumar, S. A. Kazmi and N. Yasmeen, "Comparative study of automatic generation control in traditional and deregulated power environment", *World Journal of Modelling and Simulation*, Vol. 6, No.3, pp. 189-197, 2010.
- [3]. Naimul Hasan, "Optimal Agc of Deregulated Interconnected Power System with Parallel Ac/Dc Link", *International Journal of Modern Engineering Research (IJMER)*, Vol.2, Issue.4, pp-2789-2794, 2012.
- [4]. V. Donde, M. A. Pai and I. A. Hiskens, "Simulation and optimization in an AGC system after deregulation", *IEEE Transactions on Power Systems*, Vol.16, No.3, pp.481-489, 2001.
- [5]. Mukta and Balwinder Singh Surjan, "Load Frequency Control of Interconnected Power System in Deregulated Environment: A Literature Review", *International Journal of Engineering and Advanced Technology (IJEAT)* ISSN: 2249 – 8958, Vol. 2, Issue-3, pp. 435-441, 2013.
- [6]. ElyasRakhshani and JavadSadesh, "Practical viewpoints on load frequency control problem in a deregulated power system", *Energy Conversion and Management*, Vol. 51, No. 5, pp.1148 -1156, 2010.
- [7]. Tan Wen, Zhang. H and Yu.M, "Decentralized load frequency control in deregulated environments", *Electrical Power and Energy Systems* Vol.41, pp.16-26, 2012.
- [8]. Bhatt .P, Roy.R and Ghoshal..SP, "Optimized multi area AGC simulation in restructured power systems", *Electrical Power and Energy Systems*, Vol.32, pp.311 -322, 2010.
- [9]. I.A.Chidambaram and B.Paramasivam, "Optimized Load- Frequency Simulation in Restructured Power System with Redox Flow Batteries and Interline Power Flow Controller", *International Journal of Electrical Power and Energy Systems*, Vol.50, pp 9-24, 2013.
- [10]. Sterpu,S, Besanger, Y. and Hadjsaid,N., "Ancillary services performance control in deregulated power system", *Power Engineering Society General Meeting ; IEEE*, Vol. 3, pp.3048-3054, 2005.
- [11]. J.O.P.Rahi, Harish Kumar Thakur, Abhash Kumar Singh and Shashi Kant Gupta, "Ancillary Services in Restructured Environment of Power System", *International Journal of Innovative Technology and Research (IJITR)* ISSN: 2320-5547, Vol. 1, Issue No. 3, pp.218-225, 2013.
- [12]. Dimitris Ipsakis, Spyros Voutetakis, PanosSeferlisa, FotisStergiopoulos and Costas Elmasides, "Power management strategies for a stand-alone power system using renewable energy sources and hydrogen storage", *International Journal of Hydrogen Energy*, Vol.34, pp 7081-7095, 2009
- [13]. Ke 'louwani S, Agbossou K and Chahine R, "Model for energy conversion in renewable energy system with hydrogen storage", *Journal of Power Sources* Vol.140, pp.392-399, 2005.
- [14]. P.K.Ray, S.R.Mohanty and Nand Kishor, "Dynamic Load-Frequency Control of Hybrid Renewable Energy Based Power System with HVDC-Link",

- Journal of Electrical Engineering: Theory and Application, Vol.1, Issue.1, pp.24-31, 2010
- [15]. Robin Parker and William L. Clapper, Jr, "Hydrogen - based utility energy storage system", Proceedings of the 2001 DOE Hydrogen Program Review NREL/CP-570-30535
- [16]. Surya Prakash and S.K.Sinha, "Artificial Intelligent and PI in Load Frequency Control of Interconnected Power system", International Journal of Computer Science & Emerging Technologies (E-ISSN: 2044-6004), Vol. 1, Issue 4, pp.377-384, December 2010.
- [17]. George Ellis, Control System Design Guide, 3rd Edition, Elsevier Academic Press, California, 2004
- [18]. K.M.Passino, "Biomimicry of bacterial foraging for distributed optimization and control", IEEE Control System Magazine, Vol.22, No.3, pp. 52-67, 2002.
- [19]. Janardan Nanda, Mishra.S. and Lalit Chandra Saikia, "Maiden Application of Bacterial Foraging-Based optimization technique in multi-area Automatic Generation Control", IEEE Transaction on Power System, Vol.24, No.2, pp. 602-609, 2009.
- [20]. M.Peer Mohamed, E.A.Mohamed Ali, I.Bala Kumar, "BFOA Based Tuning of PID Controller For A Load Frequency Control In Four Area Power System", International Journal of Communications and Engineering, ISSN: 0988-0382E, Vol. 3, No.3, Issue: 02, pp. 56-64, 2012.

APPENDIX - A

A1 Data for Thermal Reheat Power System [9]

Rating of each area = 2000 MW, Base power = 2000 MVA, $f^0 = 60$ Hz, $R_1 = R_2 = R_3 = R_4 = 2.4$ Hz / p.u.MW, $T_{g1} = T_{g2} = T_{g3} = T_{g4} = 0.08$ s, $T_{r1} = T_{r2} = T_{r1} = T_{r2} = 10$ s, $T_{i1} = T_{i2} = T_{i3} = T_{i4} = 0.3$ s, $K_{p1} = K_{p2} = 120$ Hz/p.u.MW, $T_{p1} = T_{p2} = 20$ s, $\beta_1 = \beta_2 = 0.425$ p.u.MW / Hz, $K_{r1} = K_{r2} = K_{r3} = K_{r4} = 0.5$, $2\pi T_{12} = 0.545$ p.u.MW / Hz, $a_{12} = -1$.

A.2 Data for the HES unit [13]

$K_{AE} = 0.002$, $T_{AE} = 0.5$, $K_{FC} = 0.01$, $T_{FC} = 4$